

# Beach geomorphic factors for the persistence of subsurface oil from the Exxon Valdez spill in Alaska

Yuqiang Xia · Michel C. Boufadel

Received: 20 July 2010 / Accepted: 27 January 2011  
© Springer Science+Business Media B.V. 2011

**Abstract** Oil from the 1989 Exxon Valdez oil spill persists in some of the Prince William Sound (Alaska) beaches and continues to be a potential threat to the fauna. This paper reports a field investigation during the summer of 2008 of groundwater flow and solute transport in a tidal gravel beach in Smith Island, Prince William Sound. The beach contains oil on one side, the left side (facing landward). Field measurements of water table, salinity, and tracer (lithium) concentration were obtained for an approximate duration of 64 h for two transects, the oiled transect and a clean transect (the right transect). It was found that the hydraulic

conductivity and the fresh groundwater recharge into the two transects were similar. It was also found that the beach slope of the mid to high tidal zone along the oiled (left) transect was  $\sim 7.4\%$  which is considerably smaller than that of the clean (right) transect ( $\sim 11.8\%$ ). This suggests a higher flushing/replenishing of the right transect with nutrients and/or oxygen, which would have enhanced biodegradation of oil on the right transect if that oil was not washed by waves. We also found that the degree of oiling at each location was inversely dependent on the armoring of the beach surface with clasts and boulders. The applied tracer concentration at the left transect was less than 2% of the source or close to the background level at all locations except a seaward well closest to the applied location, indicating that the tracer applied was diluted or washed out from the beach during the application. Thus, in situations where oil biodegradation is limited by the availability of nutrients and/or dissolved oxygen, applying the chemicals on the beach surface would most likely not enhance oil biodegradation as the applied chemicals would be greatly diluted prior to reaching the oil. Thus, deep injection of nutrients and/or dissolved oxygen is probably the only option for enhancing oil biodegradation.

---

Y. Xia · M. C. Boufadel (✉)  
Center for Natural Resources Development  
and Protection (NRDP), Department of  
Civil and Environmental Engineering,  
Temple University, 1947 N. 12th Street,  
Philadelphia, PA 19122, USA  
e-mail: boufadel@temple.edu

Y. Xia  
e-mail: xiayq@temple.edu

*Present Address:*

Y. Xia  
School of Environmental Studies &  
(MOE) Biogeology and Environmental  
Geology Lab, China University of  
Geosciences, Wuhan 430074,  
People's Republic of China

**Keywords** Field measurements · Tracer study ·  
Tidal gravel beach · Environmental pollution ·  
Oil persistence · Exxon Valdez oil spill

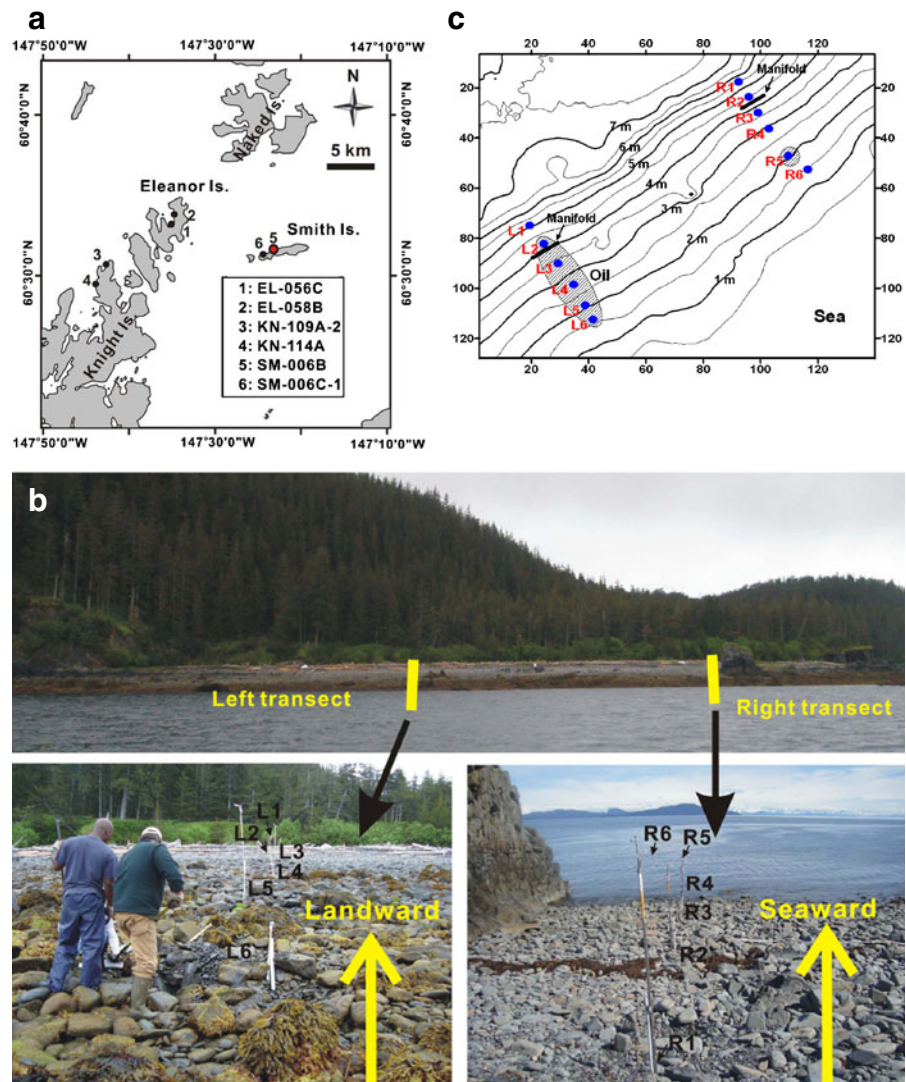
**Introduction**

In March 1989, the Exxon Valdez vessel/tanker ran aground and spilled about 41 million liters of Alaskan North Slope crude oil in Prince William Sound (PWS), Alaska. The spill polluted around 800 km of rocky intertidal shorelines within PWS (Bragg et al. 1994; Neff et al. 1995). Gibeaut and Piper (1998) measured in 1993 a total of 2,041 m<sup>3</sup> of subsurface oiled sediment in 109 locations including 738 m<sup>3</sup> of oiled sediments. They evaluated that the total length of shoreline contaminated with subsurface oil was about 7 km. Recent studies

by scientists from the National Oceanic and Atmospheric Administration (NOAA; Short et al. 2004, 2006) estimated that between 60 and 100 tons of subsurface oil persist in many initially-polluted beaches in PWS. The persistence of oil was noted by other studies (Michel and Hayes 1999; Taylor and Reimer 2008; Li and Boufadel 2010; Xia et al. 2010).

Michel et al. (2009) developed geospatial models to estimate potential areas of lingering subsurface oil from the Exxon Valdez spill on shorelines of PWS and Gulf of Alaska. They reported that the known occurrences of patches of subsurface

**Fig. 1** **a** Location of the selected beach (SM-006B) in Smith Island, PWS, Alaska (after Li and Boufadel 2010). **b** Site picture. Note that pit at L6 was being dug in this figure. **c** Topographic contours of the beach and locations of twelve observation wells. The area where the oil persists is indicated in shade. The manifold for tracer application is represented by a black bar. Well names begin with “L” for the *left* (oiled) transect and with “R” for the *right* (clean) transect. All dimensions are in meters



oil described as moderate oil residue (MOR) or heavy oil residue (HOR) extend along 1.45 km of shoreline. Their model predicted the length of shoreline oiled with HOR is 2.21 km. Xia et al. (2010) reported the persistence of the subsurface oil in a tidal gravel beach (KN-114A) on Knight Island (Fig. 1a).

To restore oiled beaches, it is necessary to have a thorough understanding of the beach hydrogeological characteristics and groundwater dynamics (Michel et al. 2006; Owens et al. 2008; Li and Boufadel 2010). Recently, Li and Boufadel (2010) presented field measurements of water table and pore water salinity in an oiled transect and a clean transect on beach EL-056C on Eleanor Island (see Fig. 1a). They found that the beach consists of two hydraulically different layers: an upper layer with a high permeability underlain by a layer whose permeability is 100 to 1,000-fold smaller. They also found that oil is present in the transect with the smaller fresh groundwater flow (flowing seaward). Boufadel et al. (2010) and Sharifi et al. (2010) confirmed the presence of low concentration of oxygen and nutrients which thus could be the limiting factor for oil biodegradation.

Taylor and Reimer (2008) reported that sites with the most extensive visibly recorded subsurface oil residues were on Smith Island, Knight Island, and Eleanor Island. The highest average total petroleum hydrocarbon concentrations were also recorded at sites Smith Island and Knight Island. Gibeaut and Piper (1998) reported that a gravel beach (SM-006B) on the north side of Smith Island retained MOR to HOR across the mid to upper intertidal zone in 1993 (see Fig. 7a in their report). The beach SM-006B is around 11 km southeast of the beach EL-056C and its coordinates are 147° 23' 6.41" W, 60° 31' 39.10" N (see Fig. 1a). Michel et al. (2006) identified this beach as the site that in 2001 contained the largest volume of oiled sediment (see Fig. 11 and Table 5 in their report), and they concluded that there has been essentially no change in the subsurface oiling on this beach since 1994. Based on data collected at shoreline segments that were surveyed between 2001 and 2008, Michel et al. (2009) reported the persistence of subsurface oil in this beach. They found that 31 of 96 pits had subsurface oil, among them 10 contained HOR and 11 contained MOR

(see Summary Sheets for SM-006B in Pooled Data Set in their report).

To provide insights into the factors affecting the subsurface lingering of the 1989 Exxon Valdez oil spill in the beach SM-006B, the present investigation reports measurements of water table, pore water salinity, and the results of a tracer study of lithium solution applied on the beach surface. The data are reported from two transects: the left transect contained oil at many locations at the level of HOR and the right transect, which was generally clean except at the most seaward measurement location (Fig. 1c). The distance between the two transects was around 90 m, thus it is unlikely that any interaction between them is occurring. Six pits were excavated in each transect and various measurements tubes were placed in them as discussed in the “Methods” section.

## Methods

Beach topography (Fig. 1c) was surveyed using an Electronic Total Station (SET330R3, SOKKIA CO. LTD, Japan). The beach slope varied as one moves seaward. Along the left transect, the beach slope was around 10% landward of L1 (13.5 m) and decreased to 7.5% seaward of L1. Along the right transect, it is ~23% between 0 and 6.5 m (landward of R1), ~11.8% between R1 and 28.0 m (R4), and ~6.4% seaward of R4. The beach surface consisted of granules (a few millimeters in size), pebbles and cobbles (10–20 cm) interdispersed between boulders (up to 100 cm) at both transects. The sediments of the beach are characterized as “boulder/cobble/gravel” shore (Page et al. 2008).

Along each transect, six pits (L1–L6 along the left transect and R1–R6 along the right transect) were hand-dug down to a depth of approximately 0.8 m whenever possible (Table 1). Oil was found under the boulders (5–30 cm below clean sediments) at wells L2–L6 (HOR at L3–L5, MOR at L2 and L6), particularly in the middle intertidal zone (Fig. 1c). Along the right transect, all pits were clean of oil except the pit of R5, which contained oil at the level of MOR. Twenty five sediment samples were obtained at various depths (from surface to ~0.8 m), and were sieved in

**Table 1** Elevations of beach surface, sensors, and ports at different locations

Locations	x(m)	Surface elevation (m)	Sensor elevation (m)	Pit depth (m)	Ports elevation (m)		
					Port A	Port B	Port C
L*1	0.0	6.96	–	–	–	–	–
L*2	6.75	6.26	–	–	–	–	–
L1	13.53	5.12	4.43	0.77	4.54	4.77	5.00
L2	22.26	4.11	3.80	0.47	3.84	4.07	–
MT	24.13	3.95	–	–	–	–	–
L3	31.50	3.31	–	0.33	3.18	3.40	–
L4	41.48	2.74	2.43	0.44	2.39	2.72	–
L5	50.72	2.03	–	0.42	1.81	2.04	–
L6	56.91	1.58	1.23	0.52	1.25	1.47	–
LTM	78.28	0.0	–	–	–	–	–
R*1	0.0	6.89	–	–	–	–	–
R1	6.54	5.39	4.90	0.49	5.33	–	–
R2	13.48	4.48	3.94	0.64	4.04	4.26	–
MT	14.81	4.33	–	–	–	–	–
R3	20.51	3.68	–	0.45	3.42	3.65	–
R4	27.90	2.88	2.51	0.70	2.36	2.59	2.82
R5	40.59	2.10	–	0.74	1.54	1.77	2.00
R6	49.35	1.52	1.25	0.31	1.40	–	–
LTM	72.42	0.0	–	–	–	–	–

L\*1, L\*2, and R\*1 are only used to control the geometry of the surface, no wells were installed at these locations. *MT* denotes the location of manifold from which the tracer was applied onto the beach surface at two transects. *LTM* is the low tide mark at this beach

the lab to generate the grain size distribution. At the left transect, the average effective grain size ( $d_{10}$ ) was 1.6 mm, the average grain size ( $d_{50}$ ) was 9.4 mm, and the average coefficient of uniformity ( $d_{60}/d_{10}$ ) was around 10, suggesting a broad grain size distribution (or poorly sorted sediments). At the right transect,  $d_{10} = 1.5$  mm,  $d_{50} = 11.2$  mm, and  $d_{60}/d_{10} = 11$ , therefore the grain size distributions along the left and right transects were similar.

In each pit, a PVC pipe and a multiport sampling well were installed vertically. The PVC pipe was already slotted across over the whole length to allow water passage. A pressure transducer (Mini-Diver, dataLogger) was placed at the bottom of the PVC pipe to record the water pressure every 10 min for a duration of 64 h (starting at 04:10 PM on June 29, 2008, taken herein as the initial time  $t = 0$  in this paper). The barometric pressure, monitored by an air-pressure sensor (BaroLogger, DL-500, Schlumberger) at the same period, was subtracted from the readings of the pressure transducers to provide the water level.

The multiport sampling wells were made of stainless steel and contained ports at various levels. The ports were spaced at the interval of  $\sim 0.23$  m and were labeled A, B, C, and D from the bottom up. Each port was connected via a tubing that extended to the top of the pipe. A tygon tube was placed on each of the tubings, and it was connected to a luer lock three-way valve. To prevent blockage by fine sediments to guarantee good hydraulic connection between the beach pore water and the water inside the well, the multiport wells were wrapped with fine stainless steel screen.

After the pit excavation for well installation, the pits were filled with the extracted sediments, which were relatively loose in comparison to the surrounding material around the pit. This provided an unwanted increase in the permeability in the pit, which was referred to as the “pit effect” in Li and Boufadel (2010) and Xia et al. (2010).

A tracer study was conducted by applying sea-water solutions of lithium nitrate (lithium was the conservative tracer) on the beach surface through

a manifold placed between L2 and L3 at the left transect and between R2 and R3 at the right transect (Table 1, Figs. 1c and 2). The manifold was a perforated 5 m long, 1.5-in. ID PVC tube that contained 2-mm orifices uniformly distributed along its whole length. The orifices were turned upward, and the uniformity of the height of water jets was achieved by adjusting the elevation of the manifold. For example, if the height of the jets was high at the right end of the manifold, then that end was raised by shimming a pebble underneath it, which caused the height of the jets at that location to decrease.

The tracer solutions were pumped from two 400-L tanks in sequence. The first tank contained a concentration of 3,390 mg/L of lithium nitrate and was used in the first 54 min, and the second tank contained a concentration of 2,130 mg/L of lithium nitrate and was used in the following 67 min. The corresponding lithium concentrations of tracer solution were 339 and 213 mg/L, respectively. The difference in concentrations was because it was not feasible to accurately measure the water volume in the tanks because they got deformed upon placement on uneven pavements. The flow rate per unit length of the 5-m long

manifold was  $75 \pm 6.8 \text{ Lh}^{-1} \text{ m}^{-1}$ . The tracer was applied on the beach surface during the falling tide. It was started at 11:59 AM ( $t = 19.82 \text{ h}$ ) on June 30, 2008. Due to the occurrences of ponding water and seepage water during the applied period, the application was stopped at 01:43 PM ( $t = 21.55 \text{ h}$ ). Then it was restarted at 04:59 PM ( $t = 24.82 \text{ h}$ ) and lasted 17 min ( $t = 25.10 \text{ h}$ ).

The lithium concentration of ponding water observed at 7 m seaward of well L2 was 264 mg/L at 01:20 PM ( $t = 21.17 \text{ h}$ , 23 min before the first application was finished). A puddle formed at 2 m seaward of well R3 at 1:30 PM ( $t = 21.34 \text{ h}$ ), its lithium concentration was 10.2 mg/L. Seepage face was detected at 5 m seaward of well L2 at 01:46 PM ( $t = 21.60 \text{ h}$ , 3 min after the first application was finished), then seepage water decreased with time and vanished at 02:29 PM ( $t = 22.31 \text{ h}$ ), its lithium concentration was 222 mg/L at 02:03 PM ( $t = 21.88 \text{ h}$ ). Ponding water of 2 cm was observed around the pit L4 at 04:00 PM ( $t = 23.83 \text{ h}$ ) and disappeared at 05:30 PM ( $t = 25.33 \text{ h}$ , 14 min after the second application was finished).

Pore water samples were obtained mainly from  $t = 20 \text{ h}$  to  $\sim 32 \text{ h}$  and from  $t = 40 \text{ h}$  to  $\sim 52 \text{ h}$  (see Figs. 6 and 7). They were approximately 40 mL,

**Fig. 2** Schematic cross-section of **a** the left transect and **b** the right transect in the beach. Well locations and tracer application location are shown here. The intersection of the high tide mark with the beach face occurs at  $x = 11.0 \text{ m}$ ,  $z = 5.47 \text{ m}$  at the left transect, and at  $x = 6.0 \text{ m}$ ,  $z = 5.47 \text{ m}$  at the right transect. The detailed information about wells and other locations is presented in Table 1

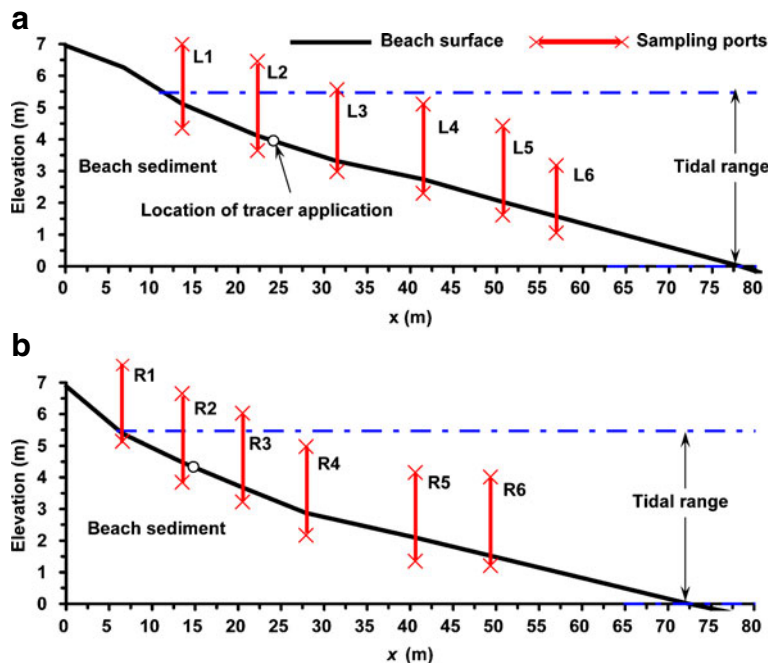


**Table 2** Fitted parameter values for tide

Harmonic component $i$	Amplitude $A_i$ (m)	Phase shift $\phi_i$ (rad)	Explanation <sup>a</sup>
1	0.522	-0.024	Main lunar diurnal (O1), $\omega_1 = 0.243$ rad/h
2	0.638	4.733	Lunar-solar diurnal (K1), $\omega_2 = 0.262$ rad/h
3	1.357	-3.281	Main lunar semidiurnal (M2), $\omega_3 = 0.506$ rad/h
4	0.440	0.365	Main solar semidiurnal (S2), $\omega_4 = 0.524$ rad/h
5	0.294	-3.203	Lunar elliptic (N2), $\omega_5 = 0.496$ rad/h
$h_{\text{MSL}} = 2.896$ m			Mean sea level

<sup>a</sup>Detailed explanations can be found in Table 4 of Merritt (2004).

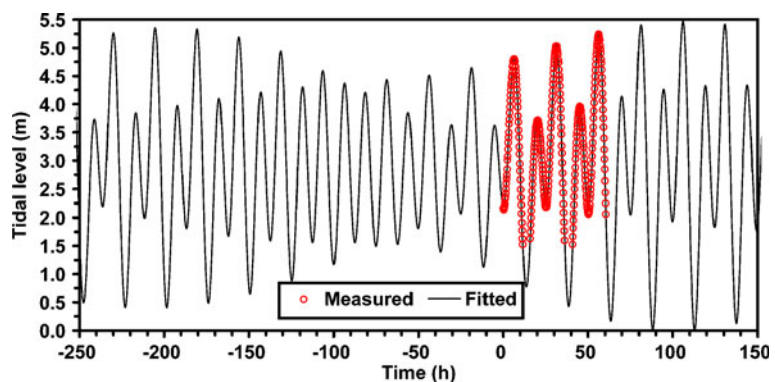
and were collected with 60-mL luer lock syringes from the multiport sampling wells and placed in 125-mL polyethylene bottles (Fischer Scientific, Fairlawn, NJ). Nitrate strips (Aquachek, Hack) whose sensitivity was 1.0 mg/L were used to measure the nitrate concentration. The sampling through syringes was stopped when the nitrate concentration, and consequently the lithium concentration, was equal to or less than 1.0% of that in the tanks. The samples were shipped to the laboratory for chemical analysis of the lithium concentration and salinity. The lithium concentrations of 197 samples (110 samples from the left transect and 87 samples from the right transect) were measured by atomic absorption spectroscopy with an air-acetylene flame at 670.8 nm (210VGP Atomic Absorption Spectrophotometer, Buck Scientific, Inc). The salinity was measured using Digital Refractometer (300035, SPER SCIENTIFIC) for each of the total 181 samples (97 samples from the left transect and 84 samples from the right transect), and then was calibrated by subtracting the tracer concentration from it for each sample.

Because we did not have pressure sensors that were capable of capturing the elevation of the low tide, we fitted a theoretical expression of tide (Merritt 2004) to the observed open water level at R6. The analytical expression was:

$$H_{\text{Tide}}(t) = h_{\text{MSL}} + \sum_{i=1}^5 A_i \cos(\omega_i t + \phi_i) \quad (1)$$

Where  $H_{\text{Tide}}$  is the tide level,  $h_{\text{MSL}}$  denotes the mean sea level, and the summation represents five harmonic components (O1, K1, M2, S2, and N2, see Table 2) for tides. The parameters  $A_i$ ,  $\omega_i$  and  $\phi_i$  are the amplitude (m), frequency (radian/hour) and phase shift (rad) of the  $i$ th component of tide, respectively. The mean sea level and the values of the five tidal components were estimated by the least square method (Table 2). Although the theoretical expression for tide contains seventeen components, experimentation with the expression (Li and Boufadel 2010) revealed that five components are sufficient. The observed and simulated tidal levels are reported in Fig. 3.

**Fig. 3** Measured water level above surface of R6 (circle symbols) and tidal level fitting result (line). Elapsed times are defined as number of hours since 04:10 PM (the started time for field monitoring works,  $t = 0$  h) on June 29, 2008. An entire spring-neap tide cycle was shown in this figure. Tidal parameter values are presented in Table 2



## Results and discussion

### Water tables

Figure 4 shows the variations of observed water table with time at four wells (L1, L2, L4, and L6) along the left transect. During falling tides, the water level at L1 kept falling at the same speed as the tide for a certain depth below the beach surface, and then it began to gradually diverge from the falling tides. Approximately 2 h later, the water level became approximately constant until the subsequent tide arrived there. The same behavior was observed at L2 except that there was no gradual change in the water table which became abruptly constant (more or less) during low tides. This behavior of water table variation indicates a two-layered hydraulic structure: a high-permeability surface layer underlain by a low-permeability lower layer. The surface layer would have a permeability so high such that the water table within it falls as fast as the falling tide. The lower layer would have a permeability so low that the water table does not drop much within it. This was also observed in the sedimentary gravel beach on Eleanor Island investigated by Li and Boufadel (2010) and in a shallow bedrock beach on Knight Island investigated by Xia et al. (2010).

The water tables at wells L4 and L6 began to diverge from the falling tides once they fell below the beach surface, and kept falling with a smaller speed until subsequent flood tide arrived, showing a different variation from that at L1 and L2. This behavior of water table variation is consistent with that observed in homogeneous beaches where the dropping velocity of the water table is more or less smooth (Nielsen 1990; Robinson and Gallagher 1999; Gibbes et al. 2008). These results indicate that there is no evidence of two layers at the two seaward wells (L4 and L6).

Figure 4 also shows that the water tables at L4 and L6 during lower low tides were lower than those during other low tides. This suggests that beach desaturation is highly dependent on the tide, which is slightly different from the work of Bobo et al. (2011) where they noted that the lowest water table elevation was independent on how low the tide was, it was basically controlled by the landward water table.

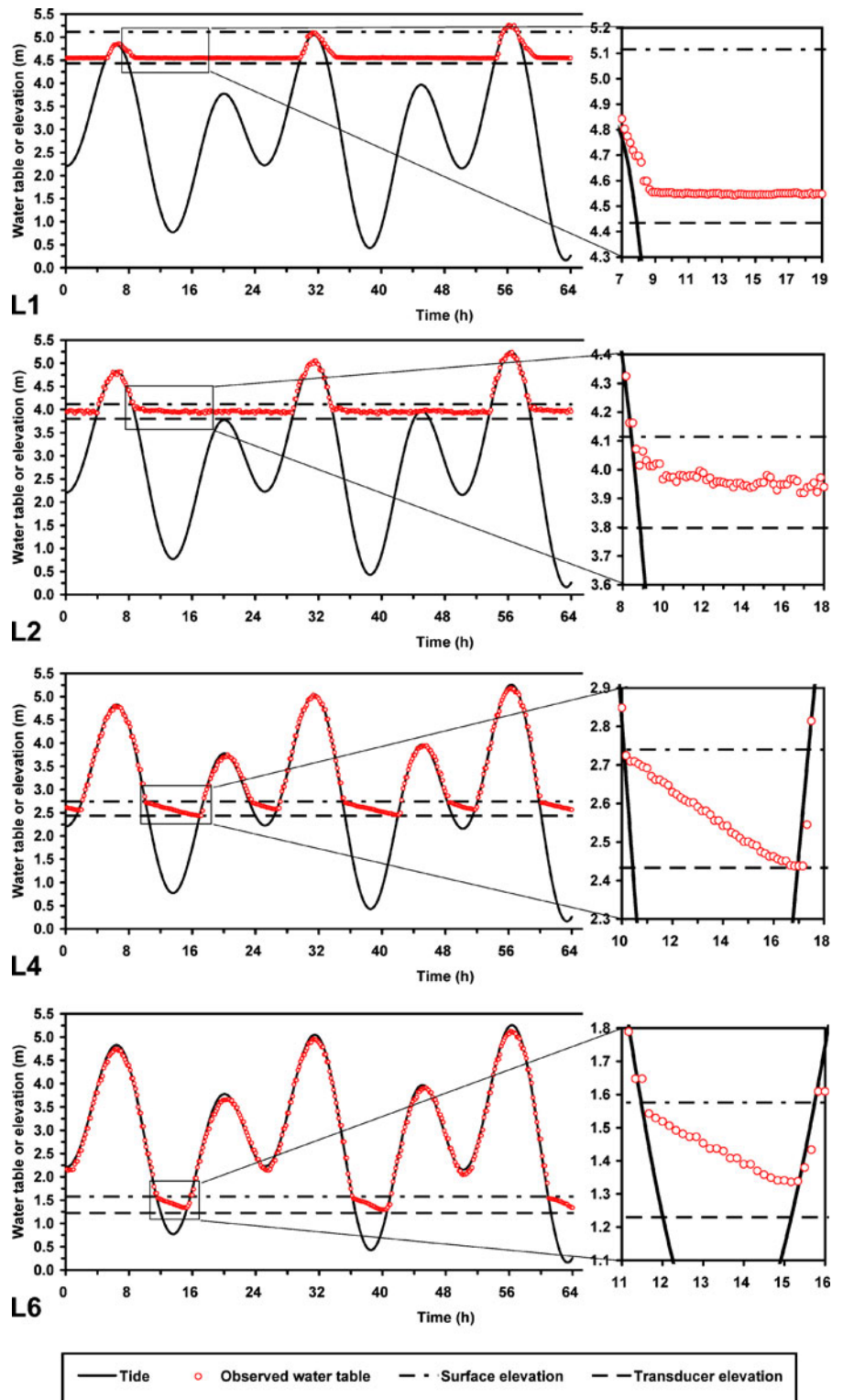
Figure 5 reports the observed water tables at wells R1, R2, R4, and R6 along the right transect. The pressures measured by the transducer at well R1 reached zero and negative pressure during low tide, which indicates that the water table dropped below the transducer's elevation. The water level at R2 began to diverge from the falling tides once they fell below the beach surface, and kept falling with a small speed until it dropped below the transducer's elevation. Nevertheless, the water tables at R1 and R2 are still reliable at higher pressures, i.e., when the water tables were higher than the transducer's elevation.

The water table at well R4 kept falling at the same speed as the tide for a certain depth (~7 cm) below the beach surface, and then became abruptly constant. Then, around 1.5 h later, the water table started falling again almost at a constant speed until subsequent flood tide arrived. This behavior indicates that the properties (e.g.,  $K$ , porosity) of sediments around R4 change with depth. The observed water table at R6 kept falling at the same speed as that of the tide for a while after the beach surface was exposed. After that, the water table elevation abruptly separated from the falling tides and was approximately constant until subsequent flood tide arrived. This phenomenon is the same as that observed at L2, and indicates the presence of two layers at that location.

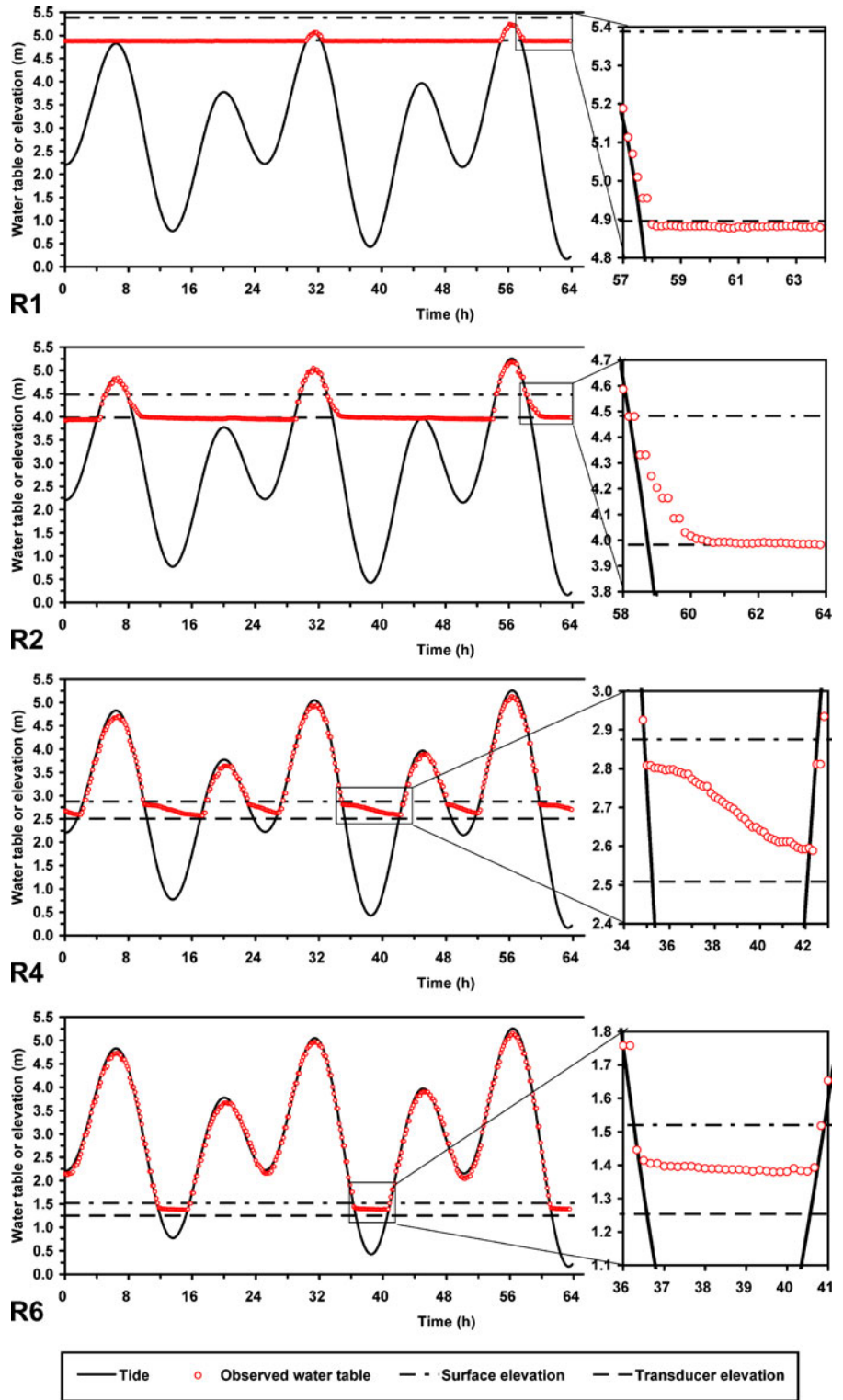
### Salinities

Figure 6 presents the variation of salinity along the left and right transects. Overall, the salinities of the two transects were essentially the same. The salinity at L1 measured during high tides ranged from 27 to 31 g/L with a mean value of 29.8 g/L. Two measurements of salinity at R1 during high tides were 24 and 25 g/L. The salinity at L2 varied significantly with tides, it ranged from 15 g/L during low tides to 36 g/L during high tides. The measurements of salinity at R2 occurred during rising tides, they increased from 32 to 35 g/L with rising tides. Most of the measured salinities at wells L3–L6 were higher than 30 g/L, and the average was 31.5 g/L with a range of 25–40 g/L. The changes of salinity at wells R3–R6 were similar to that at L3–L6, the averaged salinity was 32.2 g/L with a range of 28–39 g/L.

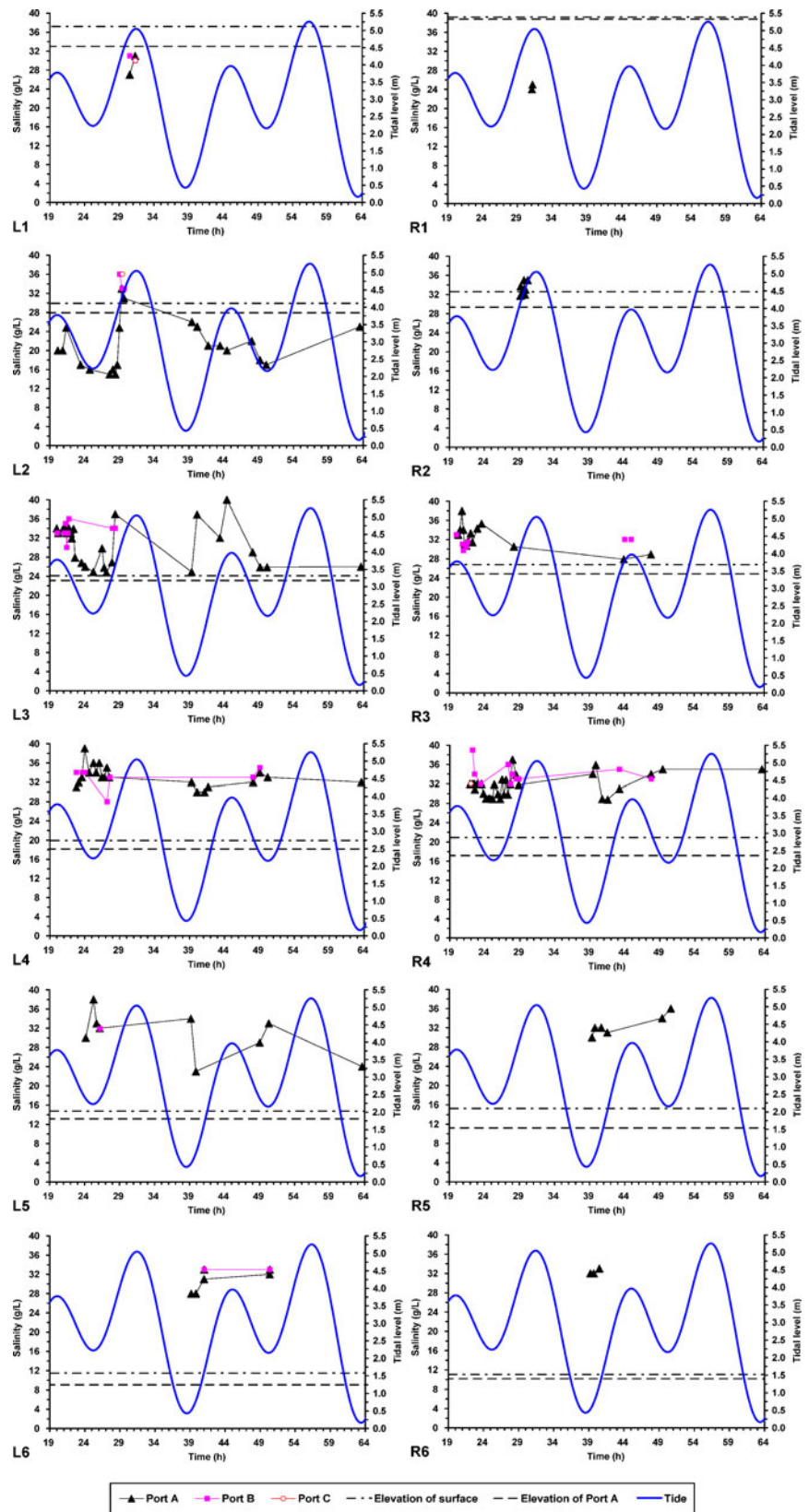
**Fig. 4** Observed water table (*circles*) at L1, L2, L4, and L6 along the left transect. The tidal level, the elevations of the beach surface and the pressure transducer installed at these observation wells are shown to indicate the submersion period



**Fig. 5** Observed water table (circles) at R1, R2, R4, and R6 along the *right* transect. The tidal level, the elevations of the beach surface and the pressure transducer installed at these observation wells are shown to indicate the submersion period



**Fig. 6** Observed salinity at ports of all wells along the *left* and *right* transects. The tidal level, the elevations of the beach surface, the elevation of the port A at these observation wells are also shown



The low pore water salinities at L2 and L3 during low tides indicate freshwater recharge from inland of the left transect. The pore water salinity at well R1 (24–25 g/L) was lower than that at wells R2–R6 (~32.3 g/L) and was also lower than that at L1 (27–31 g/L) along the left transect (Fig. 6), thus it is probable that there was freshwater recharge from the inland of the right transect.

Tracer (lithium) concentrations

Figure 7 shows the observed lithium concentrations of the pore water at different depths of wells along the left (L1–L6) and right (R1–R6) transects. No observed data were available during tracer application at L1 because the tide was too far from it to affect it. However, after the tides arrived at L1, the lithium concentration there reached a maximum of approximately 2.0 mg/L around  $t = 30$  h.

Relatively high concentrations were measured at well L2 (which was 1.87 m landward of the manifold) at two different times: One high lithium concentration (20.6 mg/L) was measured at  $t = 21.37$  h during tracer application. Another high lithium concentration (20.6 mg/L) was observed at  $t = 29.02$  h when the port A of L2 was submerged by the rising tides. Despite these two data, the lithium concentrations at L2 remained at the background level, which together with the measurements at L1 indicate that only a small landward movement of the tracer occurred. At well L3 which was 7.37 m seaward of the manifold, the lithium concentrations ranged from 0.2 mg/L to 20.3 mg/L at port A and ranged from 0.0 mg/L to 4.7 mg/L at port B. The lithium concentrations were less than 4.5 mg/L (2% of the applied concentration) at seaward wells L4, L5, and L6 during the whole monitoring period.

The observed lithium concentration at port A of well R1 was 1.5 mg/L around  $t = 31.1$  h when the port was submerged by rising tides. The lithium concentrations at port A of well R2 which was 1.33 m landward of the manifold reached its maximum (30.5 mg/L) when the port was submerged by rising tides, indicating a small landward movement of the tracer. The maximums of the lithium concentrations at well R3 which was 5.7 m seaward of the manifold were 71 mg/L at port

A and 53.2 mg/L at port B, indicating a seaward movement of the tracer. As the tracer moved seaward, its concentrations at well R4 decreased to 22.7 mg/L at port A and they were less than 2.6 mg/L at port B. These values indicate 3- to 20-fold reduction in the concentration at ports A and B, respectively going from R3 to R4. Therefore, it is highly likely that a large portion of the plume left the beach between R3 and R4. This was supported by a puddle formed at 2 m seaward of well R3 during tracer application (i.e., ease of water to leave the beach at that location). The lithium concentrations were less than 2.2 mg/L at wells R5 and R6, suggesting a very small seaward movement of the tracer between R4 and these wells.

Overall, the lithium concentrations at the left and right transect were much lower than the maximum of the applied concentration, the former was less than 21% of the latter, indicating a large dilution of the tracer.

Tracer plume movements

An integral means to quantify the overall motion of the tracer plume is tracking the variation of its centroid with time. This approach was used in prior works (Boufadel et al. 2007, 2006). Using the available ports, the coordinates of the centroid of the plume in the horizontal ( $X_G$ ) and vertical ( $Z_G$ ) directions are estimated by:

$$X_G = \frac{M_{x,1}}{M_{x,0}} \tag{2a}$$

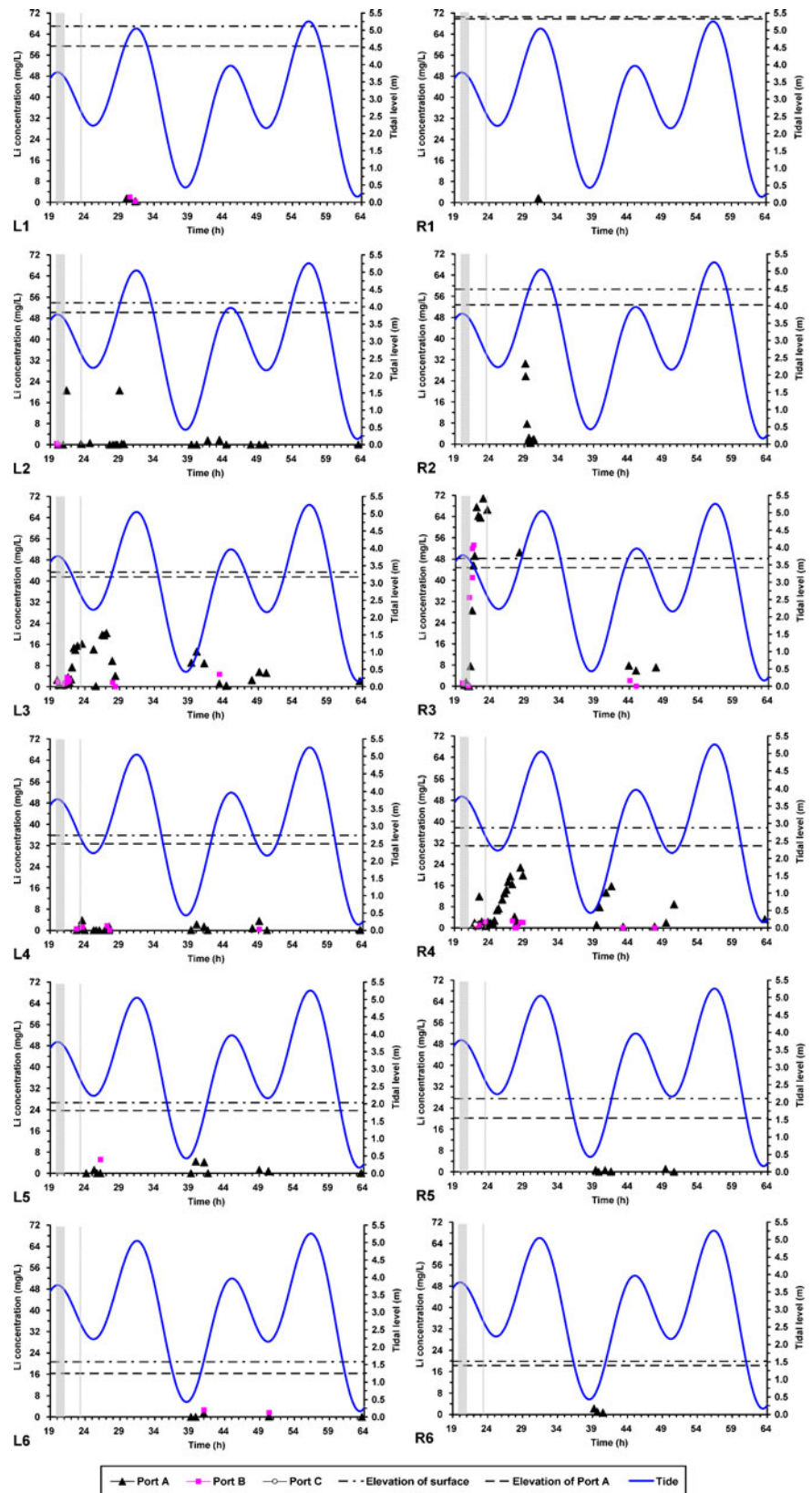
$$Z_G = \frac{M_{z,1}}{M_{z,0}} \tag{2b}$$

Where  $M$  represents the spatial moment in the  $x$  or  $z$  direction, evaluated as:

$$M_{s,q} = \sum_{i=1}^{np} s_i^q c_i, \quad q = 0 \text{ or } 1, s = x \text{ or } z \tag{3}$$

where  $x$  and  $z$  are the horizontal and vertical coordinates of the port where the concentration  $c_i$  is measured,  $np$  is the total number of ports used to compute the moments. The application of Eqs. 2a, b and 3 required interpolating linearly the concentration data with time to provide sufficient

**Fig. 7** Observed lithium (abbreviated as “Li” in the figure) concentration of the pore water at ports (labeled with ports *A*, *B*, and *C*) of all wells along the *left* and *right* transects. The tracer application started at  $t = 19.82$  h and was stopped at  $t = 21.55$  h. It was then restarted at  $t = 24.82$  h and stopped at  $t = 25.10$  h. The applied concentration of lithium was 339 mg/L during the first 54 min and 213 mg/L for 67 min. The two durations of tracer application are indicated using the *shaded bar* in this figure. The tidal level, the elevations of the beach surface, of the port *A* at these observation wells are also shown



points for the evaluation of the centroid coordinates. The results are reported in Fig. 8a and b.

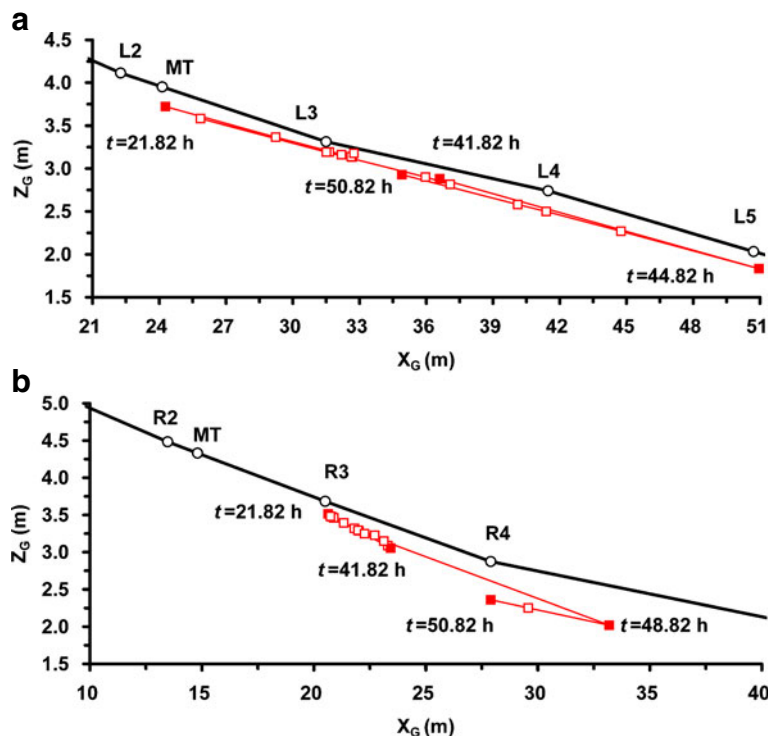
Figure 8a shows that the centroid of the plume in the left transect stayed around the applied location (MT) from  $t = 19.82$  to  $21.82$  h. However in the right transect, it moved seaward around 3 m during this period (Fig. 8b). The travel time of the peak of tracer concentration (Fig. 7) also indicates that the tracer plume took around 7.3 h moving from MT to L3 (7.4 m seaward of MT) in the left transect and 3.2 h to move from MT to R3 (5.7 m seaward of MT) in the right transect. Thus, one concludes that the plume moved slower seaward in the left transect than in the right transect during this period. This seems to explain the high dilution of the plume in the left transect in comparison with the right transect (the plume had a longer residence time in the left transect). Note also that the concentration was much lower in L3 than in R3 (see Fig. 7).

Figure 8b shows that the centroid of plume in the right transect moved only 4 m seaward of R3 from  $t = 21.82$  h to  $47.82$  h, indicating that the plume might have exited the beach between R3

and R4 which was  $\sim 7.4$  m seaward of R3. This is supported by the low tracer concentrations at R4 (3 to 20 folds reduction from R3, Fig. 7) and by an observed puddle formed at 2 m seaward of well R3 during the application. Figure 8b also shows that the centroid of the plume moved to the seaward area of R4 and dropped about 0.5 m there, which was much deeper than that at R3. This could be due to the fact that the pit depth at R4 is larger than that at R3, providing more dilution of the plume (note the lithium concentration at R3 was still around  $8.9$  mg/L at  $t = 50.52$  h, Fig. 7).

The usage of moments in computing the centroid in this work is expedient because it allows comparison of overall transport between transects. But one needs to interpret the results carefully because the centroid location is greatly affected by sensors that are far from the manifolds. Three factors could explain the difference in the movement of the tracer plumes in the two transects: (1) the hydraulic conductivity of the left transect was higher than that of the right transect, and/or (2) groundwater flow (made up of freshwater) moving seaward was larger on the left transect than on

**Fig. 8** Movements of the tracer plume centroid for **a** the left transect and **b** the right transect. Note the difference in the horizontal scale, adopted for clarity of presentations



the right transect, and/or (3) the geomorphology (i.e., large scale properties) of the two transects was different.

Regarding the first issue (hydraulic conductivity,  $K$ ), laboratory sieve analyses were conducted for sediment samples collected from two transects at different depths (see “Methods” section), and they indicated that there was no considerable difference (e.g., the same order of magnitude) between the means and variances of  $K$  values of the left and right transects. In addition, had the  $K$  value been the only factor for discrepancy, the landward motion on the left transect would have been larger than that on the right transect, because a high  $K$  value implies ease of transport of the solute plume in both the seaward and landward senses. However, the lithium concentration at L2 remained at the background level. Therefore, the hydraulic conductivity is not the reason for the difference in solute transport between the left and right transects.

Considering the second issue (groundwater flow from the land), the inland freshwater recharge can be deduced from the observed pore salinity in the two transects, which was essentially the same. Thus, the second speculation was excluded. Which leads to consider that the geomorphology was probably the reason for the difference: the beach slope of mid- to high tidal zone in the left transect is  $\sim 7.4\%$ , which is considerably smaller than that of the right transect ( $\sim 11.8\%$ ). In addition, the bedrock was essentially at the pit bottoms (where we could not longer dig), and the pit depths along the left transect were close to each other at wells L2–L5 (Table 1), indicating an approximate same depth of the beach sediments along this transect.

Thus, the left transect has a smooth bedrock of beach due to its relatively uniform beach slope. In this case, the plume’s pathway would not change much, that is why the centroid of the plume moved seaward almost parallel to the beach surface in the left transect. The beach slope along the right transect is  $\sim 11\%$  from R2 to R4 and  $\sim 6.4\%$  seaward of R4. The depth of bedrock changed considerably along the right transect (Table 1), it was 0.45 m at R3, much smaller than that at R4 and R5 ( $\geq 0.7$  m). In this case, the plume probably “dipped” going from R3 and R4, and

the small beach slope and the large depth of the pit R4 allowed the plume to penetrate deeper into the beach and to persist there. Therefore, the difference in geomorphology is the only explanation for the difference in the plume movements between two transects (Fig. 8); more precisely that the beach slope was milder and the bedrock of beach was more smooth along the left transect than along the right transect. This has desirable practical implications, as one can easily measure the beach slope and relatively easily measure the depth to bedrock (using geophysical techniques). Therefore, one could notionally predict the relative movement of solutes in beaches based on easily measured properties, precluding the need for a detailed investigation, as conducted herein.

#### Subsurface persistence of the Exxon Valdez oil

Our investigation during the summer of 2008 showed that 6 of 12 pits (L2–L6, R5) contained oil at the level of HOR or MOR, while other pits were relatively clean (Fig. 1c). Atlas and Bragg (2009) investigated 30 pits in this beach and most of which were close to the right transect, they reported that only two pits contained subsurface oil with less than 70% loss of Total PAH and other pits had no detectable subsurface oil. It is reasonable to assume that the oil loading on both transects of the beach following the Exxon Valdez oil spill in 1989 is the same considering that the transects are distant by less than 100 m.

Previous field investigations (Gibeaut and Piper 1998; Michel et al. 2006, 2009) concluded that the subsurface oil remains in this beach because it is sequestered under boulders and cobbles that provided a local wave shadow that protected the oil from removal along this high-energy beach. Hayes and Michel (1999) illustrated the armoring role of beach surface on subsurface oil lingering in gravel beaches, and listed factors enhancing the retention of the oil including mild slopes of the middle beach and a thick sediment veneer over a bedrock platform. Our synoptic survey indicated that the armoring on the left transect is much stronger than that on the right transect, which could have played a major role in sheltering the oil from the effects of waves.

Beach slope could have played a role in oil persistence. On the left transect, the beach slope was mild while the beach slope was steep on the right transect. Therefore, it is likely that the steep slope caused replenishment of the beach with nutrients and oxygen during the tidal cycle and/or wave cycles, which would have accelerated the biodegradation of oil. However, we do not believe that the steep slope caused the washout of the oil as the difference in pore water flow is too small to cause the dislodgement of oil held in place by capillary forces (at the residual content, one might need to conquer a negative pressure of 10 meters to get the oil out of the small interstices of the beach sediments).

From a biochemistry point of view, the lack of biodegradation of oil on the left transect could be due to limitations in nutrients or dissolved oxygen. The maximum concentration of nutrients in PWS is less than 0.4 mg N/L (Eslinger et al. 2001; Bragg et al. 1994; Boufadel et al. 2010; Sharifi et al. 2010), an order of magnitude lower than the concentration needed for maximum microbial growth, which ranges from 2 (sometimes 5) to 10 mg N/L (Lewis et al. 1995; Venosa et al. 1996; Boufadel et al. 1999; Wrenn et al. 2006). In addition, Li and Boufadel (2010) reported also low concentration of oxygen at oiled pits. Boufadel et al. (2010) and Sharifi et al. (2010) further confirmed that the low level of efficient electron acceptors (oxygen and nitrate) detected at the oily spots is responsible for slow and potentially inefficient biodegradation of the oil. Thus, the natural biodegradation rate of oil is expected to be slow due to the small concentrations of nutrients and dissolved oxygen.

## Conclusions

This paper presented a field study in 2008, where measurements of water table, salinity, and tracer (lithium) concentration were obtained in a tidally influenced gravel beach of PWS polluted by the 1989 Exxon Valdez oil spill. Two transects were set in the beach, a left transect (facing landward) that contained oil and a right transect. The beach slope in the mid-high tidal zone along the right

(clean) transect was  $\sim 11.8\%$ , and it was  $\sim 7.4\%$  along the left (oiled) transect. Pore water salinities indicated the same freshwater recharge from the inland into the two transects. The lithium concentrations of pore water were much lower than the applied concentration, implying a large dilution, especially in the left transect. The results showed that the centroid of the plume along the left transect moved almost parallel to the beach surface, which was attributed to the gentle beach slope and smooth bedrock of beach in that transect.

The lack of biodegradation of oil on the left transect could be due to limitations in nutrients or dissolved oxygen. The water flow in the right transect was high due to the steep slope and/or waves, which would replenish the pore water with nutrients and/or oxygen which would enhance biodegradation on the transect. In addition, the tracer concentration at the left transect was less than 2% of the source or close to the background level in all wells except the seaward well closest to the applied location, indicating that the tracer applied was diluted or washed out from the beach during the application. If one considers the tracer as nutrients or dissolved oxygen, one concludes that applying the nutrients on the beach surface would not most likely enhance oil biodegradation as the applied nutrients would greatly dilute prior to reaching the oil. Thus deep injection of nutrients and/or dissolved oxygen is probably the only option.

**Acknowledgements** This work was supported by Exxon Valdez Oil Spill Trustee Council (No. 070836). The first author was supported in part by the “111 Project” of China (No. B08030). However, it does not necessarily reflect the views of the funding entities, and no official endorsement should be inferred. We thank many Temple University faculty and students who assisted in this work.

## References

- Atlas, R. M., & Bragg, J. (2009). Bioremediation of marine oil spills: When and when not—The Exxon Valdez experience. *Microbial Biotechnology*, 2(2), 213–221. doi:10.1111/j.1751-7915.2008.00079.x.
- Bobo, A. M., Li, H. L., & Boufadel, M. C. (2011). Groundwater flow in a tidally influenced gravel beach in Prince William Sound, Alaska. *Journal of Hydrologic Engineering*, in press.

- Boufadel, M. C., Li, H. L., Suidan, M. T., & Venosa, A. D. (2007). Tracer studies in a laboratory beach subjected to waves. *Journal of Environmental Engineering*, 133(7), 722–732.
- Boufadel, M. C., Reeser, P., Suidan, M. T., Wrenn, B. A., Cheng, J., Du, X., et al. (1999). Optimal nitrate concentration for the biodegradation of *n*-heptadecane in a variably-saturated sand column. *Environmental Technology*, 20(2), 191–199.
- Boufadel, M. C., Sharifi, Y., Van Aken, B., Wrenn, B. A., & Lee, K. (2010). Nutrient and oxygen concentrations within the sediments of an Alaskan beach polluted with the Exxon Valdez oil spill. *Environmental Science & Technology*, 44(19), 7418–7424. doi:10.1021/es102046n.
- Boufadel, M. C., Suidan, M. T., & Venosa, A. D. (2006). Tracer studies in laboratory beach simulating tidal influences. *Journal of Environmental Engineering*, 132(6), 616–623. doi:10.1061/(asce)0733-9372(2006)132:6(616).
- Bragg, J. R., Prince, R. C., Harner, E. J., & Atlas, R. M. (1994). Effectiveness of bioremediation for the Exxon Valdez oil spill. *Nature*, 368, 413–418.
- Eslinger, D. L., Cooney, R. T., McRoy, C. P., Ward, A., Kline, T. C., Simpson, E. P., et al. (2001). Plankton dynamics; observed and modelled responses to physical conditions in Prince William Sound, Alaska. *Fisheries Oceanography*, 10(1), 81–96.
- Gibbes, B., Robinson, C., Li, L., Lockington, D., & Li, H. L. (2008). Tidally driven pore water exchange within offshore intertidal sandbanks: Part II numerical simulations. *Estuarine Coastal and Shelf Science*, 80(4), 472–482. doi:10.1016/j.ecss.2008.08.021
- Gibeau, J. C., & Piper, E. (1998). 1993 Shoreline oiling assessment of the Exxon Vuldez oil spill. Exxon Vuldez Oil Spill Restoration Project Final Report (Restoration Project 93038), Juneau, Alaska, Alaska Department of Environmental Conservation.
- Hayes, M. O., & Michel, J. (1999). Factors determining the long-term persistence of Exxon Valdez oil in gravel beaches. *Marine Pollution Bulletin*, 38, 92–101.
- Lewis, A., Daling, P. S., Kristiasen, T. S., Nordvik, A. B., & Fiocco, R. J. (1995). Weathering and chemical dispersion of oil at sea. In *Proceedings of international oil spill conference* (pp. 157–164). American Petroleum Institute.
- Li, H. L., & Boufadel, M. C. (2010). Long-term persistence of oil from the Exxon Valdez spill in two-layer beaches. *Nature Geoscience*, 3, 96–99. doi:10.1038/ngeo1749.
- Merritt, M. L. (2004). *Estimating hydraulic properties of the Floridian aquifer system by analysis of earth-tide, ocean-tide, and barometric effects, Collier and Hendry Counties, Florida*. *Water Resources Investigations Report 03-4267* (p. 69). Tallahassee, Florida: United States Geological Survey.
- Michel, J., & Hayes, M. O. (1999). Weathering patterns of oil residues eight years after the Exxon Valdez oil spill. *Marine Pollution Bulletin*, 38(10), 855–863.
- Michel, J., Nixon, Z., & Cotsapas, L. (2006). *Evaluation of oil remediation technologies for lingering oil from the Exxon Valdez oil spill in Prince William Sound, Alaska* (p. 47). Exxon Valdez Oil Spill Restoration Project Final Report (Restoration Project 050778), Juneau, Alaska, National Marine Fisheries Service, National Oceanic and Atmospheric Administration.
- Michel, J., Nixon, Z., Hayes, M. O., Short, J., Irvine, G., Betenbaugh, D., et al. (2009). *Modeling the distribution of lingering subsurface oil from the Exxon Valdez oil spill* (p. 121). Exxon Valdez Oil Spill Restoration Project Final Report (Restoration Project 070801), Juneau, Alaska, National Oceanic and Atmospheric Administration.
- Neff, J. M., Owens, E. H., Stoker, S. W., & McCormick, D. M. (1995). Shoreline oiling conditions in Prince William Sound following the “Exxon Valdez” oil spill. In P. G. Wells, J. N. Butler, & J. S. Hughes (Eds.), *Exxon Valdez oil spill—Fate and effects in Alaskan waters, ASTM STP 1219 American Society for Testing and Materials* (pp. 312–346). Philadelphia, PA.
- Nielsen, P. (1990). Tidal dynamics of the water table in beaches. *Water Resources Research*, 26, 2127–2134.
- Owens, E. H., Taylor, E., & Humphrey, B. (2008). The persistence and character of stranded oil on coarse-sediment beaches. *Marine Pollution Bulletin*, 56(1), 14–26.
- Page, D. S., Boehm, P. D., & Neff, J. M. (2008). Shoreline type and subsurface oil persistence in the Exxon Valdez spill zone of Prince William Sound, Alaska. In *Proceedings of the 31st Arctic and Marine Oil Spill Program (AMOP) technical seminar, Calgary, AB, Canada, 2008* (pp. 545–563). Environment Canada.
- Robinson, M. A., & Gallagher, D. L. (1999). A model of ground water discharge from an unconfined coastal aquifer. *Ground Water*, 37(1), 80–87.
- Sharifi, Y., Van Aken, B., & Boufadel, M. C. (2010). The effect of pore water chemistry on the biodegradation of the Exxon Valdez oil spill. *Water Quality, Exposure and Health*, in press. doi:10.1007/s12403-010-0033-4.
- Short, J. W., Lindeberg, M. R., Harris, P. M., Maselko, J. M., Pella, J. J., & Rice, S. D. (2004). Estimate of oil persisting on the beaches of Prince William Sound 12 years after the Exxon Valdez oil spill. *Environmental Science & Technology*, 38(1), 19–25.
- Short, J. W., Maselko, J. M., Lindeberg, M. R., Harris, P. M., & Rice, S. D. (2006). Vertical distribution and probability of encountering intertidal Exxon Valdez oil on shorelines of three embayments within Prince William Sound, Alaska. *Environmental Science & Technology*, 40(12), 3723–3729.
- Taylor, E., & Reimer, D. (2008). Oil persistence on beaches in Prince William Sound—A review of SCAT surveys conducted from 1989 to 2002. *Marine Pollution Bulletin*, 56, 458–474.
- Venosa, A. D., Suidan, M. T., Wrenn, B. A., Strohmeier, K. L., Haines, J., Eberhart, B. L., et al. (1996). Bioremediation of an experimental oil spill on the shoreline of Delaware Bay. *Environmental Science & Technology*, 30, 1764–1775.

Wrenn, B. A., Sarnecki, K. L., Kohar, E. S., Lee, K., & Venosa, A. D. (2006). Effects of nutrient source and supply on crude oil biodegradation in continuous-flow beach microcosms. *Journal of Environmental Engineering*, 132, 75–84.

Xia, Y. Q., Li, H. L., Boufadel, M. C., & Sharifi, Y. (2010). Hydrodynamic factors affecting the persistence of the Exxon Valdez oil in a shallow bedrock beach. *Water Resources Research*, 46, W10528. doi:[10.1029/2010WR009179](https://doi.org/10.1029/2010WR009179).